Stem Cell Reports
Resource
OPEN ACCESS

Identifying Division Symmetry of Mouse Embryonic Stem Cells: Negative Impact of DNA Methyltransferases on Symmetric Self-Renewal

Lukasz Jasnos,[1] Fatma Betül Aksoy,[1,2] Hersi Mohamed Hersi,[1] Slawomir Wantuch,[1] and Tomoyuki Sawado[1,*]
[1]Haemato-Oncology Research Unit, Division of Molecular Pathology, Division of Cancer Biology, The Institute of Cancer Research, Sutton SM2 5NG, UK
[2]Present address: Department of Molecular Biology and Genetics, Boğaziçi University, Bebek 34342, Istanbul, Turkey
*Correspondence: tomoyuki.sawado@icr.ac.uk
http://dx.doi.org/10.1016/j.stemcr.2013.08.005

SUMMARY

Cell division is a process by which a mother cell divides into genetically identical sister cells, although sister cells often display considerable diversity. In this report, over 350 sister embryonic stem cells (ESCs) were isolated through a microdissection method, and then expression levels of 48 key genes were examined for each sister cell. Our system revealed considerable diversities between sister ESCs at both pluripotent and differentiated states, whereas the similarity between sister ESCs was significantly elevated in a 2i (MEK and GSK3b inhibitors) condition, which is believed to mimic the ground state of pluripotency. DNA methyltransferase 3a/3b were downregulated in 2i-grown ESCs, and the loss of DNA methyltransferases was sufficient to generate nearly identical sister cells. These results suggest that DNA methylation is a major cause of the diversity between sister cells at the pluripotent states, and thus demethylation per se plays an important role in promoting ESC's self-renewal.

INTRODUCTION

Stem cell divisions resulting in alternative pathways of self-renewal or differentiation require very distinctive epigenetic regulation of gene expression from the same genome. Where division has a symmetrical output of progeny cells, the assumption is that the molecular signatures derived from sister cells (daughter cells from a common parent cell) are identical. In this context, various types of markers and biological functions have been used to evaluate the symmetry of cell divisions (Beckmann et al., 2007; Huang et al., 1999; Muramoto et al., 2010; Punzel et al., 2002; Suda et al., 1983; Wu et al., 2007; Zwaka and Thomson, 2005). Although each of these studies addressed a particular biological question (e.g., similarity levels of transcriptional oscillation of a few genes between *Dictyostelium* sister cells [Muramoto et al., 2010]) and provided important information to relevant fields, the overall level of similarity between sister cells has not been thoroughly addressed. Human ESCs, for example, are considered to divide and differentiate "symmetrically" regardless of the cultural condition, but this assumption is based on the distribution of the expression of a single gene *POU5F1* measured through the signal of highly stable protein, eGFP (Zwaka and Thomson, 2005). More comprehensive and sensitive approaches should be undertaken to evaluate the actual level of division symmetry. (In this report, the term "symmetric division" refers to the generation of two daughter cells that exhibit high-level similarities in cell fates, proliferative capacities, and/or the presence of biomarkers.)

Although murine embryonic stem cells (ESCs) in culture look morphologically similar, a subset of genes is often differentially expressed within a population (Carter et al., 2008; Chambers et al., 2007; Hayashi et al., 2008; Kalmar et al., 2009; Payer et al., 2006; Singh et al., 2007). Nanog and Gata 6 proteins are expressed heterogeneously in both ESCs and the inner cell mass of E3.5 blastocysts, suggesting that the heterogeneity is not solely an in vitro phenomenon (Chazaud et al., 2006). These results raise the possibility that the fidelity of ESC "self-renewal" is less than one would predict.

Here, we established a method to isolate single sister cells through microdissection to evaluate the symmetry of ESC divisions at molecular levels. High-throughput RT-PCR analyses using isolated single sister cells suggests that ESCs divided symmetrically at the ground state of pluripotency, which was induced by a 2i condition (Ying et al., 2008), whereas the symmetry was significantly declined in pluripotent (medium with LIF and BMP4) and differentiation states (medium without LIF and BMP4). We also found that the ground pluripotent state (medium with 2i, LIF, and BMP4) was accompanied by the reduction in the number of coregulating genes at single-cell levels. Importantly, we found that DNA methyltransferases 3a and 3b (*Dnmt3a/3b)* are downregulated in 2i-grown ESCs as reported recently (Leitch et al., 2013), and ESCs that are deficient for three DNA methyltransferases generated nearly identical sister cells, suggesting the link between epigenetic regulation and the fidelity of cell divisions. We believe that our systems will expand the capability of single-cell analyses and will help identifying mechanisms that cause cellular heterogeneity, which emerges as an important problem in stem cell biology, translational research, and effective cancer treatment.

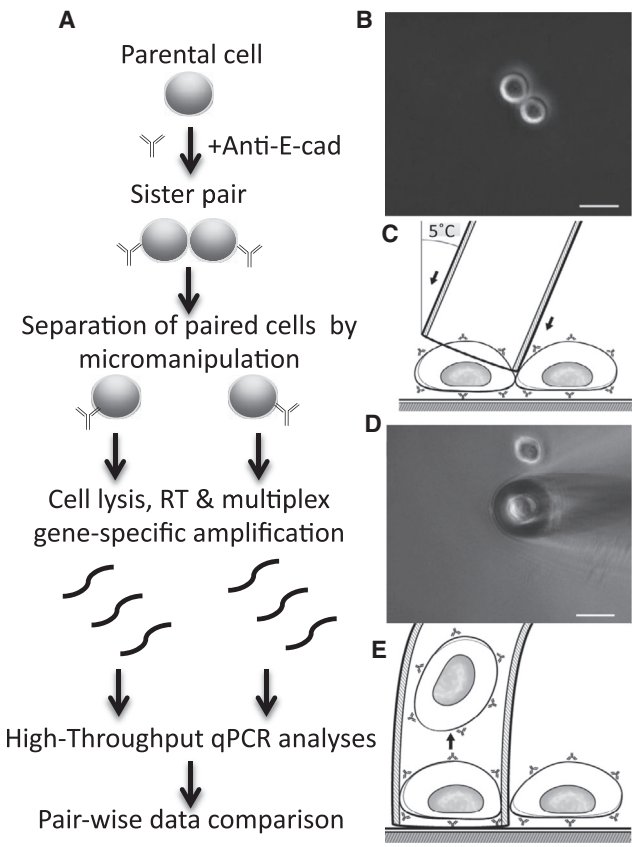

Figure 1. Single Sister Cell Analyses

(A) Procedures to evaluate the fidelity of cell division by analyzing RNA levels in each sister cell. Anti-E-cadherin (anti-E-cad) was added to keep cells in suspension. Lists of genes and primer information are described in Table S2 and S3, respectively.

(B) A pair of sister cells before the sister cell microdissection.

(C) Paired sister cells were separated by providing physical pressure on the junction between sister cells using a glass pipette.

(D) Sister cells were separated by the glass pipette.

(E) Each sister cell was recovered by altering the temperature of the glass pipette. After one of the sister cells was transferred to AG480F slide, Quixell system automatically brought back the pipette to the first picking position, and the other sister cell could be isolated and transferred.

Scale bars, 20 μm. See also Figure S1, Tables S1, S2, and S3, and Movie S1.

RESULTS

Single Sister Cell Analyses

To evaluate the similarity levels between sister ESCs, we initially compared the expression levels of two ESC markers, *Pou5f1* (also known as *Oct4*) and *Klf4*, between sister cells through single molecule FISH methods enabling each mRNA molecule to be visualized under the microscope (Raj and Tyagi, 2010). We found that whereas a few sister pairs clearly displayed considerable differences in the number of RNA spots between sister cells, a majority of pairs displayed the nearly identical number of *Klf4* RNA spots (Figure S1 available online). Although the number of *Pou5f1* RNA spots looks more inconsistent between sister cells (Figure S1), the Kolmogorov-Smirnov (K-S) test found no significant difference between *Klf4* and *Pou5f1* in the diversity levels between sister cells ($D = 0.4$, $N_{pau5f1} = 10$, $N_{klf4} = 9$, $p = 0.4$). Probe sequences are shown in Table S1. Although this method allowed us to determine the number of RNA spots for a few markers in each sister cell, the analytical process of the experiment was labor intensive and time consuming, and thus it was very difficult to analyze larger numbers of cell samples with numerous probes. These problems lead us to develop a method to evaluate the overall similarity between sister cell using high-throughput RNA analyses.

To this end, we first established a system to isolate and analyze two sister ESCs that are associated with each other at the postmitotic phase (Figure 1A). The most challenging part was to break the firm interaction between sister cells without damaging them. The Quixell automated cell transfer system (Stoelting) allowed us to isolate single cells with a glass micropipette under the microscope; however, the instrument was originally designed to isolate a "loner" single cell in suspension culture, and thus we needed to develop a protocol with the instrument to separate paired sister ESCs.

To facilitate dissecting dividing ESCs, cells were treated with nocodazole briefly, harvested, and then incubated for 90 min in fresh media containing anti-E-cadherin, which maintains cells' suspension state without compromising pluripotency even after 24 hr of labeling (Mohamet et al., 2010). We verified that anti-E-cadherin treatment (for 90 min) does not affect expression levels of 48 genes that we examined in this study ($\bar{r} = 0.99$, Figure S2A). Correlating with the previous finding that nocodazole does not alter ESC's potentials to reprogram somatic cells into pluripotent cells (Hezroni et al., 2011), a short-term incubation with nocodazole did not affect cell's undifferentiation states, which were measured based on alkaline phosphatase staining and colony morphologies (Figures S2B and S2C). We dissected paired sister ESCs (Figure 1B) by trapping one sister cell within the cylinder of a glass micropipette (10–15 μm diameter), simultaneously providing physical pressure onto the junction between sister cells with the edge of the glass micropipette (Figures 1C and 1D; Movie S1). The trapped cell can enter into the cylinder following a reduction in the temperature of the glass pipette (Figure 1E; Movie S1). Isolated single cells were quickly transferred onto a reaction site on the AmpliGrid AG480F glass slide, which allows us to monitor the integrity of the single cell optically during micromanipulation.

Table 1. Distribution of Correlation Coefficients of Expression Levels

	Valid N	Mean	Median	Min	Max	SD	CV
ESC RNA	1081	0.92	0.92	0.82	0.98	0.026	0.028
WT, +LIF	48	0.74	0.74	0.47	0.90	0.104	0.14
WT, +LIF nonsister	44	0.72	0.72	0.45	0.86	0.097	0.13
WT, - LIF	48	0.73	0.75	0.32	0.91	0.161	0.22
WT, 2i	42	0.82	0.84	0.51	0.94	0.116	0.14
WT, 2i nonsister	42	0.76	0.78	0.64	0.87	0.067	0.088
TKO, +LIF	46	0.88	0.89	0.70	0.94	0.057	0.064
Dnmt1 null, +LIF	86	0.80	0.84	0.36	0.94	0.116	0.15

Min, minimum; Max, maximum; CV, coefficient of variation. See also Figure S3 and Tables S2, S3, and S4.

Cells deposited onto the slide were then manually transferred to PCR tubes and then were frozen on dry ice. The Quixell system records the initial picking position, allowing us to isolate the other sister cell easily.

Isolated single cells were processed for cell lysis, reverse transcription, target-specific complementary DNA (cDNA) amplification, and high-throughput qPCR analyses on the Biomark HD platform. We initially selected 93 genes that are expressed in undifferentiated ESCs based on previous microarray studies (see Experimental Procedures for details). After testing primer qualities at single-cell levels, we focused on 48 target genes, which include 31 genes associated with DNA/chromatin/RNA binding including core induced pluripotent stem cell (iPSC) reprogramming factors (Takahashi et al., 2006), four genes for cytoskeleton-related proteins, five genes for metabolism/transport related proteins, two genes for cyclin-dependent kinases, four genes for membrane receptor/extracellular cytokines, and two genes for proteins with unknown molecular functions. Further details for each gene and primer sequence can be found in Tables S2 and S3, respectively. For each of 48 primer sets, we determined the higher threshold of the quantification cycle (Cq) values (Table S3), which provide good reproducibility and are still in the area of logarithmic amplification. Forty-eight replicates of the whole reaction (reverse transcription, gene amplification, and qPCR), using single-cell equivalent 30 pg of ESC RNA displayed very strong correlations among Cq values ($\bar{r}$ = 0.92), assuring the accuracy of our experimental system (Figure S2D; Table 1). It should also be noted that using the same amplified cDNA sample two independent Biomark qPCR experiments (48 × 48) displayed strong correlation between results ($\bar{r}$ = 0.98), indicating the reproducibility of the experimental approach (Figures S2E and S2F).

Pluripotent and Differentiating ESCs Do Not Generate Identical Sister Cells, but 2i Elevates ESC's Division Symmetry

Expression analyses for these 48 genes in 48 cells (24 pairs of sister cells) suggest significant transcriptional differences between sister cells even in the presence of LIF and BMP4, a combination of which supports pluripotency in culture (the pluripotent state) (Ying et al., 2003) and strong staining for alkaline phosphatase activity (Figure S3A). When cells were grown in medium with LIF and BMP4, the mean correlation coefficients ($\bar{r}$) of 48 gene expression levels based on Cq values between sister cells (total 24 pairs) was 0.74 (Table 1; Figure 2A). We also collected nonsister cells (= daughter cells originating from different parental cells) as a "pseudo" pair and then determined the similarity of gene expression levels between those two cells ($\bar{r}$ = 0.72) (Table 1; Figure 2A). Although the correlation coefficient between sister cells was slightly higher compared to nonsister cells from "pseudo" pairs, the K-S test found no significant difference between them in the presence of LIF and BMP4 (D = 0.22, $N_{\text{sister cells:+LIF\&BMP4}}$ = 48, $N_{\text{nonsister cells (pseudo pairs):+LIF\&BMP4}}$ = 44, p = 0.603). Removal of LIF and BMP4 from the media for 1 day reduced *Nanog* and *Klf4* expression (Figure S3B), and the same media caused the loss of alkaline phosphatase staining (Figure S3A) but did not alter the mean correlation coefficient value based on Cq values between sister cells ($\bar{r}$ = 0.73) (Figure S3C; Table 1). Although the measure of variance of correlation coefficients was higher in cells without LIF and BMP4 (coefficient of variation = 0.22) compared to cells in medium with LIF and BMP4 (coefficient of variation = 0.14), the K-S test found no significant difference in distribution of correlation coefficients (D = 0.21, $N_{\text{sister cells:LIF\&BMP4}}$ = 48, $N_{\text{sister cells: no LIF\&BMP4}}$ = 48, p = 0.622)(Table 1). These data suggest that at the early stage of ESC differentiation initiated by LIF withdrawal, the similarity of sister ESCs was not significantly altered.

Recently, Smith's group and others have identified and characterized several chemical compounds that could maintain ESCs at the ground state of pluripotency. PD0325901, a potent and selective inhibitor for phosphorylation of ERK, efficiently reduces spontaneous differentiation when it is combined with a GSK3 inhibitor CHIR99021 (Ying et al., 2008) or LIF (Silva et al., 2008). Co-treatment with PD0235901 and LIF reduces the expression heterogeneity of Nanog, with the increase of mean and maximum levels of expression. CHIR99021, a highly selective inhibitor for GSK3 (Murray et al., 2004) (Bain et al., 2007), promotes nonneural differentiation, but when combined with PD0325901 (2i) ESCs are not only well expanded with maintaining pluripotency (Ying et al., 2008), but also express a subset of ESC regulators more ubiquitously (Miyanari and Torres-Padilla, 2012; Wray

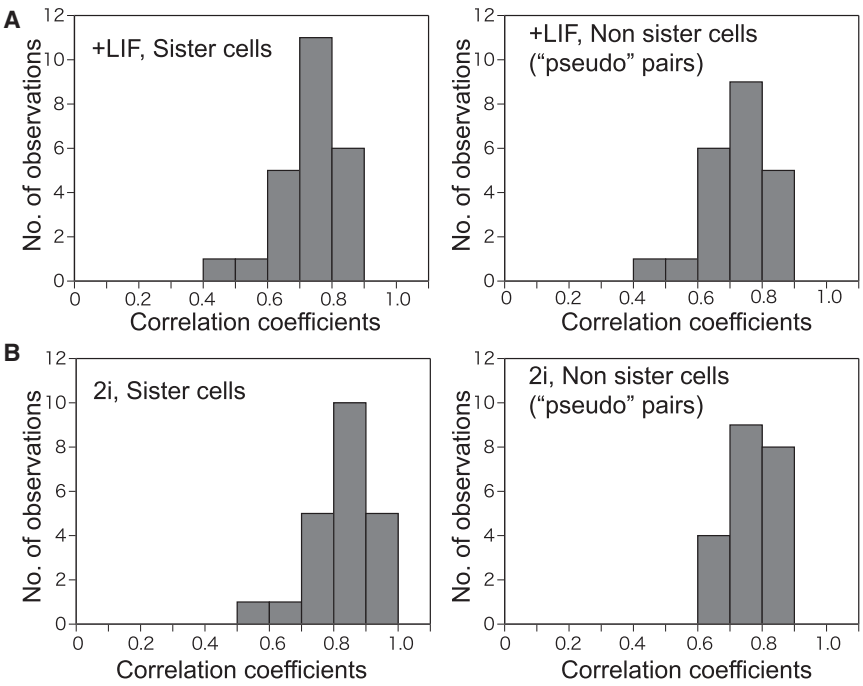

Figure 2. Similarity Levels between Sister ESCs

(A and B) Correlation coefficients of expression levels of 48 ESC markers between sister cells or nonsister cells ("pseudo" pairs) cultured in media with LIF and BMP4 (A) and with LIF, BMP4, and 2i (B).

See also Figure S2 and Tables S2, S3, and S4.

et al., 2010; Marks et al., 2012), suggesting that the pluripotency can be stabilized at the ground state with 2i treatment. When ESCs were cultured in 2i conditions, a combination of which also supported strong alkaline phosphatase staining (Figure S3A), the similarity between sister cells in 2i media was significantly elevated compared to sister cells cultured with LIF and BMP4 only ($\bar{r}$ = 0.82) (D = 0.46, $N_{\text{sister cells:2i}}$ = 42, $N_{\text{sister cells:LIF\&BMP4}}$ = 48, p = 0.01) (Figure 2B; Table 1). Correlating with this, we found differences between Cq values in a subset of genes (e.g., *Bcor*, *Klf4*, and *Nr0b1)* obtained from each sister cell were considerably reduced by 2i (Table S4). Importantly, in 2i conditions the similarity between sister cells was also significantly elevated compared to nonsister cells derived from "pseudo" pairs ($\bar{r}$ = 0.76)(D = 0.48, $N_{\text{sister cells:+2i}}$ = 42, $N_{\text{nonsister cells (pseudo pairs):+2i}}$ = 42, p = 0.011) (Table 1; Figure 2B). These results suggest that 2i reduces the levels of dissimilarity between sister cells, thereby helping to elevate the expression homogeneity of the population. Taken together, these results suggest that despite the common assumption that pluripotent ESCs proliferate through "self-renewal" cycles, they do not always produce identical sister cells based on RNA profiles. The term "self-renewal" may be more applicable to 2i conditions, because 2i significantly elevates the levels of the similarity between sister cells compared to other states. The whole expression data can be found in Table S4.

Interestingly, we found that in nonsister single cells expression levels of genes encoding reprogramming factors (*Klf4*, *Pou5f1*, and *Sox2*) correlated stronger or more significantly in media containing LIF and BMP4 compared to medium without LIF and BMP4 or 2i medium (Figure 3). We observed similar trends in 1,128 possible gene pairs, observing that adding 2i reduced the overall number of genes that are significantly correlated ($p < 0.000042$, see Table S5) compared to ESCs cultured LIF and BMP4 only (pluripotent states) after conducing the sequential Bonferroni correction for multiplicity of comparisons (Sokal and Rohlf, 2012) (Figure S4; Table S5). Interestingly, *Nanog* expression levels were not significantly correlated with a majority of genes including reprogramming factors regardless of culture conditions used. This is consistent with previous observations that *Nanog* expression levels appeared to be regulated in a stochastic manner (Kalmar et al., 2009), or are regulated through additional mechanisms not involving the other reprogramming factors (Abranches et al., 2013; Niwa et al., 2009). These results suggest that despite the greater similarity between sister cells in 2i conditions, overall levels of coordinated expression of genes including four reprogramming factors appear to be less prominent compared to the pluripotent state.

Loss of Three DNA Methyltransferases Promotes Symmetric Divisions

Recent results suggest that de novo methyltransferases *Dnmt3a/3b* were downregulated in the presence of 2i, leading to global demethylation in ESC genome (Leitch et al., 2013). The 2i condition affects gene sets that are also

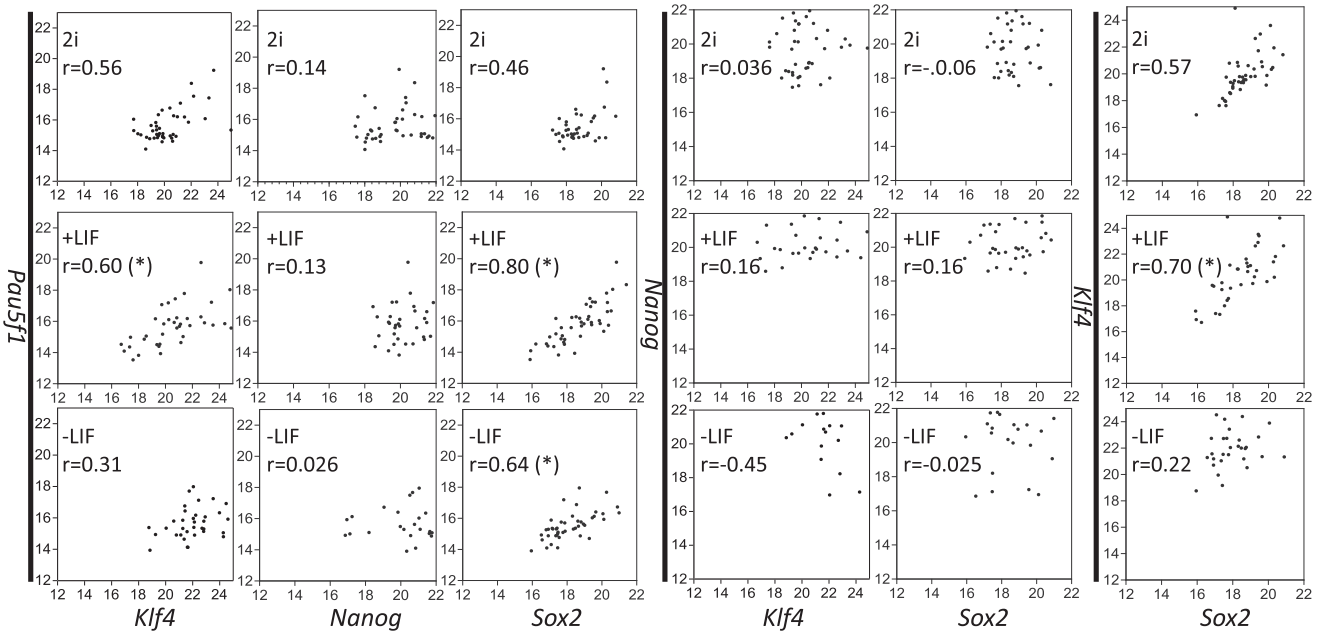

Figure 3. 2i Undermines Coregulation between Reprogramming Factors

Correlation of expression levels among reprogramming factors at single-cell levels. Both x and y axes represent Cq values of corresponding genes. Correlation coefficients (r) are shown, and the ones that are statistically significant after applying the Bonferroni correction tests are marked with an asterisk. Events with Cq values higher than the threshold (= non or low expressors) were not plotted because they were not reliable and thus were not used for statistical analyses.

See also Figure S4 and Tables S2, S3, S4, and S5.

affected by the deletion of three DNA methyltransferases, *Dnmt1*, *Dnmt3a*, and *Dnmt3b* (triple knockout = TKO [Tsumura et al., 2006; Leitch et al., 2013]). TKO ESCs display complete demethylation and can be expanded indefinitely in pro-undifferentiation ESC media (Tsumura et al., 2006). Although these results suggest the involvement of DNA demethylation in maintaining cell's ground pluripotent states, it was not clear whether demethylation promotes symmetric self-renewal, or simply reduces subpopulations that are spontaneously differentiated through cell death or slow growth (Sakaue et al., 2010; Tsumura et al., 2006).

To evaluate the link between DNA demethylation and self-renewal, we first examined the expression levels of DNA methyltransferases in ESCs through conventional RT-PCR. As recently reported by Leitch et al. (2013), we found that *Dnmt1* expression levels were relatively unchanged among three conditions, but *Dnmt3a* and *3b* were considerably downregulated in 2i-grown ESCs compared to ESCs grown with or without LIF and BMP4 (Figure 4A). Because we found that 2i-grown ESCs frequently generate symmetric sister ESCs, next we examined if the loss of DNA methyltransferases is sufficient to promote ESC's symmetric self-renewal at the pluripotent states. We cultured TKO ESCs in LIF and BMP4 media, isolated 46 sister cells, and then conducted Biomark analyses. We observed a prominently high level of similarity between sister cells in TKO backgrounds ($\bar{r}$ = 0.88)(Figure 4B; Tables 1 and S4). It should be noted that this number is close to the system's upper detection limit, $\bar{r}$ = 0.92 (Table 1), at the single-cell level. The K-S test found that the difference between wild-type and TKO ESCs is statistically significant (D = 0.70, $N_{\text{sister cells:wild-type: LIF\&BMP4}}$ = 48, $N_{\text{sister cells:TKO:LIF\&BMP4}}$ = 46, p = 0.00005). We also analyzed *Dnmt1*-null ESCs that express *Dnmt3a/3b* at normal levels (Lei et al., 1996; Tsumura et al., 2006), and the K-S test found that the similarity level was significantly reduced to $\bar{r}$ = 0.80 (D = 0.49, $N_{\text{sister cells:}Dnmt1\text{: LIF\&BMP4}}$ = 86, $N_{\text{sister cells:TKO:LIF\&BMP4}}$ = 46, p = 0.001) (Figure 4B; Tables 1 and S4). The difference of $\bar{r}$ between wild-type and *Dnmt1*-null ESCs was also statistically significant (D = 0.34, $N_{\text{sister cells:wild-type}}$ = 48, $N_{\text{sister cells:}Dnmt1\text{ null}}$ = 86, p = 0.01). These results suggest the negative impact of three DNA methyltransferases on ESCs' symmetric self-renewal. We found no prominent deregulation of ESC reprogramming factors (*Nanog*, *Sox2*, *Klf4*, and *Pou5f1*) in the TKO background (Figure 4C), suggesting that the promotion of symmetric division is caused by mechanisms other than the stimulation of regulatory circuits that those reprogramming factors are involved in. Taken together, these results imply that DNA methylation per se is one of the major

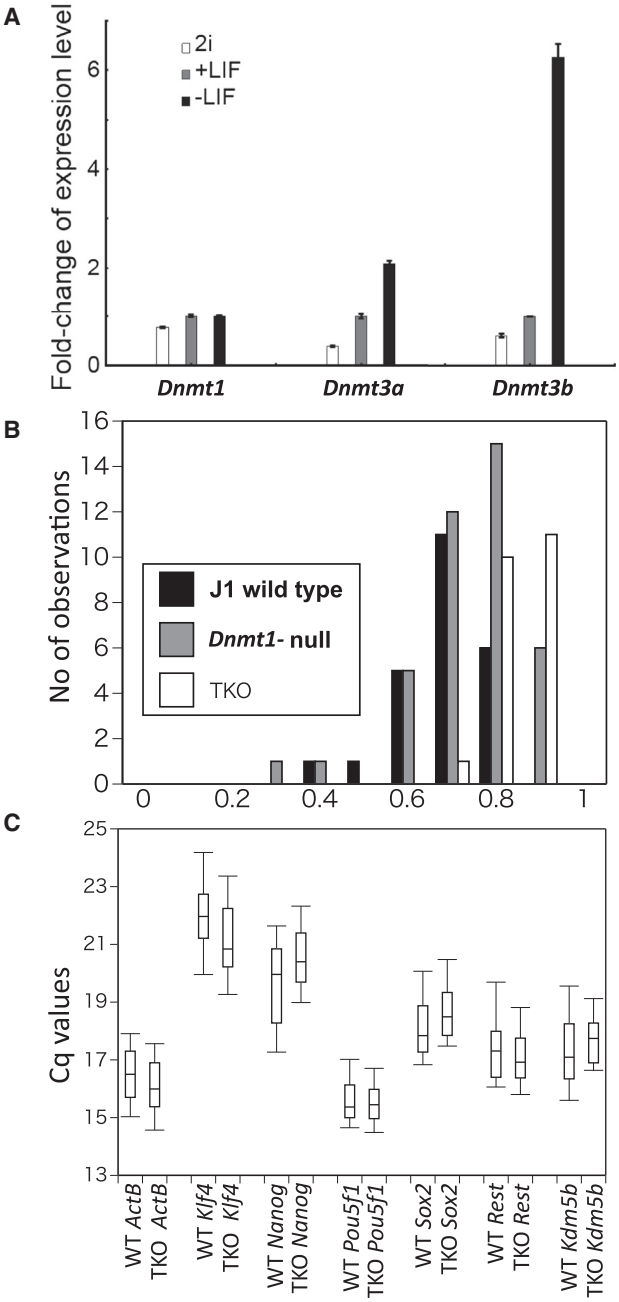

Figure 4. Deletion of Three DNA Methyltransferases Generates Nearly Identical Sister Cells

(A) Analyses of expression levels of three DNA methyltransferases using bulk RNA samples. Data plotted are fold change of expression levels in 2i- (white bars), +LIF&BMP4- (light shaded gray bars), and –LIF&BMP4- (dark shaded gray bars) grown ESCs. The SEM for two independent experiments is shown.

(B) Distributions of correlation coefficients of expression levels of 48 ESC markers between sister ESCs are plotted. The difference between WT (black bars) and TKO ESCs (white bars), WT and *Dnmt1*-null ESCs, or *Dnmt*-null (shaded gray bars) and TKO ESCs was statistically significant (see text).

(C) Box and whisker plots for expression levels of reprogramming factors in WT and TKO single ESCs are shown. Median, 25th and 75th percentile (box), and 5th and 95th percentile (whisker) are shown. See also Tables S2, S3, and S4.

causes of generating the diversity between sister ESCs, and thus the reduction or loss of DNA methyltransferase activities helps promote symmetric self-renewal.

DISCUSSION

Although the similarity between sister cells can be evaluated through imaging analyses, they are often labor intensive and thus are not suitable to process a large number of cells using multiple marker probes. In order to obtain a high-throughput data set, we processed each of over 350 sister cells to a series of molecular reactions and were able to identify a possible cause of generating the diversity between sister cells. Importantly, the microdissection method can be combined with other single-cell methodologies including analyses for genomic DNA sequence (Zong et al., 2012), CpG methylation (Kantlehner et al., 2011), noncoding and coding RNA sequence (Tang et al., 2010; Tang et al., 2006), and protein analyses (Shi et al., 2012). Sister cells isolated with this method are also viable and, thus, can be used for a series of functional analyses, such as the evaluation of proliferation kinetics and differentiation potentials.

In this report, we used a high-throughput PCR-based platform to examine the similarity between sister cells due to the difficulty to conduct RNA sequencing analyses for each of over 350 single-cell samples. Interestingly, the average correlation coefficient (0.74) observed for WT ESCs in our system appears to be slightly lower than the value from 12 randomly picked nonsister ESCs that were previously measured based on RNA sequencing (Tang et al., 2010). The difference is unlikely to be caused by low reproducibility of experimental processes in our assay systems, because our systems also provided the very high correlation coefficient when TKO ESCs were analyzed. It should be noted that there are considerable differences between two experimental systems, such as in culture conditions (ESCs cultured without or with feeder cells), cDNA amplification methods, the numbers of samples that were processed (over 40 single cells or 12 single cells), and the numbers of target genes that were analyzed (48 or over 10,000 genes). The latter factor may particularly be critical, because our system essentially focused on 48 key ESC regulators, a majority of which are factors related to transcription, whereas the other analyzed over 10,000 genes that include numerous genes that are constitutively expressed. It should be noted that the half-life of mRNA molecules for transcription factors is much shorter than the average (Sharova et al., 2009), and thus

our system could reveal the sister cell diversity, which is undetectable when the whole transcriptome is compared. Regardless of the differences in experimental conditions, our system successfully detect the diversity between sister cells, revealing intrinsic and extrinsic mechanisms that affect the mode of division symmetry of ESCs.

The role of expression noise-induced transition between cellular states has been extensively discussed in the context of differentiation (Chang et al., 2008; Furusawa and Kaneko, 2012; Pina et al., 2012). Our Biomark data suggest that cellular states of ESCs are not entirely stable even at the pluripotent state, frequently diversifying expression levels between sister cells. The expression diversity between sister cells at the pluripotent state is in part caused by DNA methylation and could be further enhanced by the coregulation network, which contributes to generate cells with more "transitional" states. A recent finding suggested that both serum-grown and 2i-grown ES cells have similar differentiation potentials (Marks et al., 2012). Similarly, a recent paper using the Biomark system suggested that multipotent hematopoietic cells do not display the presence of transcriptome fluctuation in the self-renewing cell population (Pina et al., 2012). These results suggest that, whereas transitional states are correlated with differentiation, they are unlikely to be essential for the maintenance of cell's stemness. In 2i-grown ESCs at the ground pluripotent state, undermined gene regulatory networks reduce the chance of generating cells with "transitional" states, potentially suppressing the diversity between sister ESCs. Although further improvements in the technological feasibility of next-generation RNA sequencing for single-cell assay applications may help in validating these hypotheses, this work demonstrates the clear case where the fidelity of stem cell division is examined using high-throughput assay systems.

Although it still remains to be determined whether DNA demethylation in TKO ESCs reduces the heterogeneity of the general population elevating the similarity between sister cells or directly promotes symmetric divisions, our results using 2i-grown ESCs suggest that the downregulation of DNA methyltransferases is correlated with the elevation of symmetric divisions. It has been shown that ESCs that are deficient for DNA methyltransferases grow robustly and maintain undifferentiation characteristics (Tsumura et al., 2006). This is likely to be achieved through two mechanisms at cell population levels. First, undifferentiated TKO cells gain growth advantages over differentiating TKO ESCs, which display increasing levels of growth defect and apoptotic cell death (Sakaue et al., 2010; Tsumura et al., 2006). Second, as suggested in this report, the level of symmetric division is greatly promoted by demethylation, which also takes place in 2i-grown ESCs (Leitch et al., 2013). Taken together, these results suggest that global DNA demethylation is not only antagonistic to differentiation, but also plays a role in promoting self-renewal to maintain cells at the most naive state.

EXPERIMENTAL PROCEDURES

Cells and Culture Conditions

Mouse wild-type J1 and *Dnmt1*-null J1 ESCs were obtained from Dr. Taiping Chen (MD Anderson Cancer Center). TKO J1 ESCs were obtained from Dr. Masaki Okano (Riken Institute, Japan). ESCs were cultured in DMEM/F12 media supplemented with N2, B27 (Invitrogen), BMP4 (R&D Systems), and LIF (Millipore) as described (Ying et al., 2003). 2i, a MEK inhibitor PD0325901, and a GSK3 beta inhibitor CHIR99021 were obtained from Selleckchem and Merck, respectively. Cells were treated with 0.1 μg/ml Nocodazole for 6 hr and were harvested using Accutase (Millipore), and then 0.5–1.0 × 10^4 cells were seeded in a 3.5 cm plate containing fresh media with 4 μl/ml of anti-E-cadherin, clone DECMA-1 (Sigma-Aldrich). For differentiation, LIF and BMP4 were removed from the media for 20 hr before treating with Nocodazole and then released for 90 min in the same media. Sister cells (and nonsister cells) were ready to be picked up between 90 and 180 min from the release of G2/M phase arrest. Alkaline Phosphatase staining was performed as described in the instruction manual of Alkaline Phosphatase Detection Kit (Millipore).

Imaging

Images shown in Figures 1, S2B, S2C, and S3A as well as Movie S1 were taken on an Olympus XM10 camera on an Olympus CKX41 inverted fluorescent microscope system (auto-exposure function, CELL^D [Olympus]). Cell ejection portions were omitted from Movie S1.

Sister Cell Isolation for Single-Cell Analyses

The Quixell system was installed on a CKX41 inverted microscope (Olympus). The micropipette (tip size 10–15 μm, taper length 14–18 μm, Stoelting) was slowly lowered so that only one of sister cells could be trapped within the cylinder. The trapped sister cell was allowed to enter into the pipette either through capillary action or by reducing the temperature of the pipette operated through the Quixell console. Then, 1.5 μl of loading mix (2 × reaction buffer [Cells Direct Kit, One step qPCR kit, Invitrogen]: DNA suspension buffer [Teknova]: RT-PCR grade Water [Ambion] = 5:1.3:1) was quickly added to a new reaction site of the AG480F slide, and the cell was ejected into the loading mix. Cell/loading mix was transferred from the AG480F reaction site to a PCR tube. The reaction site was washed with loading mix three times using the same pipette tip, and then washing solution was mixed with cell/loading mix in the tube (the total volume 7.3 μl). We also isolated "pseudo" pairs that are composed of two nonsister single cells, which were not located nearby. They were isolated approximately every 10 min from cultures.

Selection of Primers for cDNA Amplification

We initially designed 93 primers that cover genes that are (1) upregulated in undifferentiated ESCs (Sharova et al., 2007) including

iPSC reprogramming factors (Takahashi et al., 2006), (2) upregulated in differentiated ESCs (Sepulveda et al., 2008), heterogeneously expressed in ES colonies (Carter et al., 2008), or (3) DNMT1 target genes (GSE10519), and/or bivalent genes (Bernstein et al., 2006) (Fouse et al., 2008; Whyte et al., 2012). We rejected 23 primer sets that did not satisfy our primer validation tests (see data validation). Out of 70 genes, we decided to focus on 48 genes that provide higher frequencies of generating reliable data in test experiments. We did not include primers for development or differentiation-related genes (e.g., bivalent genes) in the final list, due to low reliability of expression data (their expression levels were too low for single-cell assays).

Reverse Transcription and Target-Specific Amplification

Samples were briefly spun down, quickly frozen on dry ice, and then stored in a −80°C freezer. Samples were then thawed on ice to disrupt the cell membrane. Reverse transcription and target-specific cDNA amplification was performed in a single-tube reaction using CellsDirect One-step qRT PCR kit (Invitrogen). A reaction mixture (0.2 μl SuperScript II RT/Platinum Taq Mix [Invitrogen] and 2.5 μl of primer mixtures for 93 genes [200 nM for each] [Deltagene Assays, Fluidigm] that were resuspended in DNA Suspension Buffer [Teknova]) was added to each tube. The reaction was incubated at 50°C for 15 min, 95°C for 2 min, followed by 18 cycles of (95°C for 15 s and 60°C for 4 min) and held at 4°C. Unincorporated primers were subsequently removed by treating with Exonuclease I (EXO I), NEB. A reaction mixture contains 10 μl of amplified cDNA, 0.4 μl of 10 × ExoI buffer, 0.8 μl EXOI enzyme (20 U/μl), and 2.8 μl of RT-PCR grade water. Reaction was held at 37°C for 30 min and then at 80°C for 15 min to inactivate of EXO I. Finally, DNA suspension buffer (36 μl) was added to each sample (total 50 μl).

Analyses Using Biomark System

Sample and primer mixtures were loaded separately to inlets located on both sides of the 48 × 48 Gene Expression Arrays (Fluidigm). A Biomark qPCR mix was composed of 2.5 μl of 2 × TaqMan Gene Expression Master Mix (Applied Biosystems), 0.25 μl of 20 × DNA Binding Dye Sample Loading Reagent (Fluidigm), 0.25 μl of 20 × EvaGreen DNA binding dye (Biotium), and 2 μl of EXO-I-treated cDNA sample. A primer reaction mix was composed of 2.5 μl of 2 × assay loading reagent, 1.25 μl of DNA suspension buffer, and 1.25 μl of a 20 μM primer pair. Sample loading was done according to the instruction manual of the Biomark system.

Expression Analyses of Anti-E-Cadherin-Treated and Untreated Cells

Five thousand ESCs were incubated with 4 μl of anti-E-cadherin for 90 min, and then RNA was prepared using TRIzol (Invitrogen). RNA (1 ng) was processed to reverse transcription, target-specific cDNA amplification, and Biomark analyses as described above.

Data Validation

All the analysis of raw qPCR data together with initial data validation was performed using Real-Time PCR Analysis Software version 3 (Fluidigm). A threshold for Cq value (Table S3) was set manually for each primer pair based on qPCR tests. Then, melting curves were analyzed to reject primer sets that produce nonspecific products. Then, a scatterplot for correlation between peaks of melting curve versus Cq value was drawn for every primer pair. Most of the primers displayed a single peak of melting curve with few distinct outliers. Based on the plot, a window of reliability for melting temperature was determined, and all of the data outside of the window were rejected from the analysis. If a particular primer pair generated a broad distribution of melting curve peaks, the primer would also be rejected from the analysis, as it produces unreliable data. We did not conduct reference gene normalization, because it is not regarded to be valid or applicable in single-cell RNA assays (Ståhlberg et al., 2013).

RT-PCR Analyses for DNA Methyltransferases

RNA samples (50 ng) were processed for RT-qPCR analyses using KAPA SYBR FAST One-Step qRT-PCR Kits (KAPABIOSYSTEMS). qPCRs were conducted on a 7900HTqPCR system (ABI). The following primers were used: *Dnmt3a*, 5′-GAC TCT CCA GAG GCC TGG TT-3′, 5′-GGC TCA CAC CTG AGC TGT ACT-3′; *Dnmt3b*, 5′-GCG ACA ACC GTC CAT TCT TC-3′, 5′-CTC TGG GCA CTG GCT CTG ACC-3′. *Dnmt1* primers are described in Table S3.

Statistical Analysis

It should be noted that Cq values higher than the threshold for reliable Cq values (Table S3) were omitted from the statistical analyses used in this paper. To evaluate the similarity of sister cells, correlation coefficients (r) for the expression levels of 48 genes between sister cells were estimated. The Kolmogorov-Smirnov test was used to evaluate the differences of correlation coefficient distributions of data sets derived from two sample sets (e.g., sister and non-sister cells), due to the presence of skewness of the distribution and uneven number of observations between compared groups, both of which were not suitable for conducting stronger tests. To find out which genes are coexpressed at a statistically significant level, we build a matrix of comparison with 48 × 48 gene combinations. Correlation between each pair of genes was computed. α-Level for statistical significance was adjusted according to the sequential Bonferroni correction for multiplicity of comparisons (Sokal and Rohlf, 2012) to avoid the elevation of type I error.

Single Molecule FISH

Stellaris RNA FISH oligoprobes (5′TAMRA labeled) for *Klf4* and *Pou5f1* were synthesized by Biosearch Technologies. Probe sequences are available in Table S1. After the release from G2 phase arrest, cells were cultured on a poly-D-lysine^{+} laminin-coated glass slide for 2 hr and then were fixed with 3.7% formaldehyde solution. Fixed cells were hybridized as described in previous reports (Raj and Tyagi, 2010; Raj et al., 2008). Forty z-sections of images with 0.2 μm spacing were taken by an LSM 700 AxioObserver Z1 confocal microscope with Plan-Apochromat 63×/1.4 oil differential interference contrast objective lens (Zeiss). To count the number of RNA spots in each sister cells using the MATLAB software, we first prepared images where one of sister cells were eliminated manually by Adobe Photoshop paintbrush tool. To remove pixel noises and enhance RNA spots, we applied a Laplacian of Gaussian

(LoG) filter (bandwidth = 9) to each z-section (Raj et al., 2008) (Raj and Tyagi, 2010), and then a z-stack was generated by Z projector (standard deviation) in ImageJ. RNA spots were then counted through the MATLAB software with image processing toolbox (MathWorks) (Raj et al., 2008) (Raj and Tyagi, 2010).

SUPPLEMENTAL INFORMATION

Supplemental Information includes four figures, five tables, and one movie and can be found with this article online at http://dx.doi.org/10.1016/j.stemcr.2013.08.005.

ACKNOWLEDGMENTS

This work was supported by funding from the ICR. F.B.A. was supported by the Erasmus Work Placement Programme. We thank Drs. Taiping Chen (MD Anderson Cancer Center) for providing J1 WT and *Dnmt1*-null ESCs and Masaki Okano (Riken) for providing TKO ESCs. We thank Dr. Johanna Jim (ICR) for experimental assistance. We thank Ms. Chi Ying Kimi Wong (ICR and Kimi Design) for the illustration used in Figure 1. We thank Professors Mark Groudine (Fred Hutchinson Cancer Research Center) and Mel Greaves and Drs Arthur Zelent, Tony Ford, and Lyndal Kearney (ICR) for critical reading and discussion. We thank Dr. Richard Mills (Stoelting) for technical support for Quixell Automated System. We thank Drs. Marc Unger (Fluidigm), Nicola Potter, Ian Titley, and Miss Gowri Vijayaraghavan (ICR) for technical advice on single-cell analyses, Dr. Christopher Wardell (ICR) for statistical analysis of microarray data. We thank Professor Ryszard Korona (Jagiellonian University in Krakow) for advice on statistical analyses. We thank Professor Sanjay Tyagi (UMDNJ) for advices and discussion on our single molecule FISH data. L.J. performed experiments, analyzed data, and wrote the paper. F.B.A. and H.M.H. performed experiments and analyzed data. S.W. performed the experiments. T.S. conceived, designed, and performed experiments, analyzed data, and wrote the paper.

Received: May 31, 2013
Revised: August 15, 2013
Accepted: August 16, 2013
Published: September 26, 2013

REFERENCES

Abranches, E., Bekman, E., and Henrique, D. (2013). Generation and characterization of a novel mouse embryonic stem cell line with a dynamic reporter of Nanog expression. PLoS ONE *8*, e59928.

Bain, J., Plater, L., Elliott, M., Shpiro, N., Hastie, C.J., McLauchlan, H., Klevernic, I., Arthur, J.S., Alessi, D.R., and Cohen, P. (2007). The selectivity of protein kinase inhibitors: a further update. Biochem. J. *408*, 297–315.

Beckmann, J., Scheitza, S., Wernet, P., Fischer, J.C., and Giebel, B. (2007). Asymmetric cell division within the human hematopoietic stem and progenitor cell compartment: identification of asymmetrically segregating proteins. Blood *109*, 5494–5501.

Bernstein, B.E., Mikkelsen, T.S., Xie, X., Kamal, M., Huebert, D.J., Cuff, J., Fry, B., Meissner, A., Wernig, M., Plath, K., et al. (2006). A bivalent chromatin structure marks key developmental genes in embryonic stem cells. Cell *125*, 315–326.

Carter, M.G., Stagg, C.A., Falco, G., Yoshikawa, T., Bassey, U.C., Aiba, K., Sharova, L.V., Shaik, N., and Ko, M.S. (2008). An in situ hybridization-based screen for heterogeneously expressed genes in mouse ES cells. Gene Expr. Patterns *8*, 181–198.

Chambers, I., Silva, J., Colby, D., Nichols, J., Nijmeijer, B., Robertson, M., Vrana, J., Jones, K., Grotewold, L., and Smith, A. (2007). Nanog safeguards pluripotency and mediates germline development. Nature *450*, 1230–1234.

Chang, H.H., Hemberg, M., Barahona, M., Ingber, D.E., and Huang, S. (2008). Transcriptome-wide noise controls lineage choice in mammalian progenitor cells. Nature *453*, 544–547.

Chazaud, C., Yamanaka, Y., Pawson, T., and Rossant, J. (2006). Early lineage segregation between epiblast and primitive endoderm in mouse blastocysts through the Grb2-MAPK pathway. Dev. Cell *10*, 615–624.

Fouse, S.D., Shen, Y., Pellegrini, M., Cole, S., Meissner, A., Van Neste, L., Jaenisch, R., and Fan, G. (2008). Promoter CpG methylation contributes to ES cell gene regulation in parallel with Oct4/Nanog, PcG complex, and histone H3 K4/K27 trimethylation. Cell Stem Cell *2*, 160–169.

Furusawa, C., and Kaneko, K. (2012). A dynamical-systems view of stem cell biology. Science *338*, 215–217.

Hayashi, K., Lopes, S.M., Tang, F., and Surani, M.A. (2008). Dynamic equilibrium and heterogeneity of mouse pluripotent stem cells with distinct functional and epigenetic states. Cell Stem Cell *3*, 391–401.

Hezroni, H., Tzchori, I., Davidi, A., Mattout, A., Biran, A., Nissim-Rafinia, M., Westphal, H., and Meshorer, E. (2011). H3K9 histone acetylation predicts pluripotency and reprogramming capacity of ES cells. Nucleus *2*, 300–309.

Huang, S., Law, P., Francis, K., Palsson, B.O., and Ho, A.D. (1999). Symmetry of initial cell divisions among primitive hematopoietic progenitors is independent of ontogenic age and regulatory molecules. Blood *94*, 2595–2604.

Kalmar, T., Lim, C., Hayward, P., Muñoz-Descalzo, S., Nichols, J., Garcia-Ojalvo, J., and Martinez Arias, A. (2009). Regulated fluctuations in nanog expression mediate cell fate decisions in embryonic stem cells. PLoS Biol. *7*, e1000149.

Kantlehner, M., Kirchner, R., Hartmann, P., Ellwart, J.W., Alunni-Fabbroni, M., and Schumacher, A. (2011). A high-throughput DNA methylation analysis of a single cell. Nucleic Acids Res. *39*, e44.

Lei, H., Oh, S.P., Okano, M., Jüttermann, R., Goss, K.A., Jaenisch, R., and Li, E. (1996). De novo DNA cytosine methyltransferase activities in mouse embryonic stem cells. Development *122*, 3195–3205.

Leitch, H.G., McEwen, K.R., Turp, A., Encheva, V., Carroll, T., Grabole, N., Mansfield, W., Nashun, B., Knezovich, J.G., Smith, A., et al. (2013). Naive pluripotency is associated with global DNA hypomethylation. Nat. Struct. Mol. Biol. *20*, 311–316.

Marks, H., Kalkan, T., Menafra, R., Denissov, S., Jones, K., Hofemeister, H., Nichols, J., Kranz, A., Stewart, A.F., Smith, A., and Stunnenberg, H.G. (2012). The transcriptional and epigenomic foundations of ground state pluripotency. Cell *149*, 590–604.

Miyanari, Y., and Torres-Padilla, M.E. (2012). Control of ground-state pluripotency by allelic regulation of Nanog. Nature *483*, 470–473.

Mohamet, L., Lea, M.L., and Ward, C.M. (2010). Abrogation of E-cadherin-mediated cellular aggregation allows proliferation of pluripotent mouse embryonic stem cells in shake flask bioreactors. PLoS ONE *5*, e12921.

Muramoto, T., Müller, I., Thomas, G., Melvin, A., and Chubb, J.R. (2010). Methylation of H3K4 Is required for inheritance of active transcriptional states. Curr. Biol. *20*, 397–406.

Murray, J.T., Campbell, D.G., Morrice, N., Auld, G.C., Shpiro, N., Marquez, R., Peggie, M., Bain, J., Bloomberg, G.B., Grahammer, F., et al. (2004). Exploitation of KESTREL to identify NDRG family members as physiological substrates for SGK1 and GSK3. Biochem. J. *384*, 477–488.

Niwa, H., Ogawa, K., Shimosato, D., and Adachi, K. (2009). A parallel circuit of LIF signalling pathways maintains pluripotency of mouse ES cells. Nature *460*, 118–122.

Payer, B., Chuva de Sousa Lopes, S.M., Barton, S.C., Lee, C., Saitou, M., and Surani, M.A. (2006). Generation of stella-GFP transgenic mice: a novel tool to study germ cell development. Genesis *44*, 75–83.

Pina, C., Fugazza, C., Tipping, A.J., Brown, J., Soneji, S., Teles, J., Peterson, C., and Enver, T. (2012). Inferring rules of lineage commitment in haematopoiesis. Nat. Cell Biol. *14*, 287–294.

Punzel, M., Zhang, T., Liu, D., Eckstein, V., and Ho, A.D. (2002). Functional analysis of initial cell divisions defines the subsequent fate of individual human CD34(+)CD38(-) cells. Exp. Hematol. *30*, 464–472.

Raj, A., and Tyagi, S. (2010). Detection of individual endogenous RNA transcripts in situ using multiple singly labeled probes. Methods Enzymol. *472*, 365–386.

Raj, A., van den Bogaard, P., Rifkin, S.A., van Oudenaarden, A., and Tyagi, S. (2008). Imaging individual mRNA molecules using multiple singly labeled probes. Nat. Methods *5*, 877–879.

Sakaue, M., Ohta, H., Kumaki, Y., Oda, M., Sakaide, Y., Matsuoka, C., Yamagiwa, A., Niwa, H., Wakayama, T., and Okano, M. (2010). DNA methylation is dispensable for the growth and survival of the extraembryonic lineages. Curr. Biol. *20*, 1452–1457.

Sepulveda, D.E., Andrews, B.A., Asenjo, J.A., and Papoutsakis, E.T. (2008). Comparative transcriptional analysis of embryoid body versus two-dimensional differentiation of murine embryonic stem cells. Tissue Eng. Part A *14*, 1603–1614.

Sharova, L.V., Sharov, A.A., Piao, Y., Shaik, N., Sullivan, T., Stewart, C.L., Hogan, B.L., and Ko, M.S. (2007). Global gene expression profiling reveals similarities and differences among mouse pluripotent stem cells of different origins and strains. Dev. Biol. *307*, 446–459.

Sharova, L.V., Sharov, A.A., Nedorezov, T., Piao, Y., Shaik, N., and Ko, M.S. (2009). Database for mRNA half-life of 19 977 genes obtained by DNA microarray analysis of pluripotent and differentiating mouse embryonic stem cells. DNA Res. *16*, 45–58.

Shi, Q., Qin, L., Wei, W., Geng, F., Fan, R., Shin, Y.S., Guo, D., Hood, L., Mischel, P.S., and Heath, J.R. (2012). Single-cell proteomic chip for profiling intracellular signaling pathways in single tumor cells. Proc. Natl. Acad. Sci. USA *109*, 419–424.

Silva, J., Barrandon, O., Nichols, J., Kawaguchi, J., Theunissen, T.W., and Smith, A. (2008). Promotion of reprogramming to ground state pluripotency by signal inhibition. PLoS Biol. *6*, e253.

Singh, A.M., Hamazaki, T., Hankowski, K.E., and Terada, N. (2007). A heterogeneous expression pattern for Nanog in embryonic stem cells. Stem Cells *25*, 2534–2542.

Sokal, R.R., and Rohlf, J.F. (2012). Biometry: the principles and practice of statistics in biological research, Fourth Edition (New York: W. H. Freeman and Company).

Ståhlberg, A., Rusnakova, V., Forootan, A., Anderova, M., and Kubista, M. (2013). RT-qPCR work-flow for single-cell data analysis. Methods *59*, 80–88.

Suda, T., Suda, J., and Ogawa, M. (1983). Single-cell origin of mouse hemopoietic colonies expressing multiple lineages in variable combinations. Proc. Natl. Acad. Sci. USA *80*, 6689–6693.

Takahashi, K., Ichisaka, T., and Yamanaka, S. (2006). Identification of genes involved in tumor-like properties of embryonic stem cells. Methods Mol. Biol. *329*, 449–458.

Tang, F., Hajkova, P., Barton, S.C., Lao, K., and Surani, M.A. (2006). MicroRNA expression profiling of single whole embryonic stem cells. Nucleic Acids Res. *34*, e9.

Tang, F., Barbacioru, C., Bao, S., Lee, C., Nordman, E., Wang, X., Lao, K., and Surani, M.A. (2010). Tracing the derivation of embryonic stem cells from the inner cell mass by single-cell RNA-Seq analysis. Cell Stem Cell *6*, 468–478.

Tsumura, A., Hayakawa, T., Kumaki, Y., Takebayashi, S., Sakaue, M., Matsuoka, C., Shimotohno, K., Ishikawa, F., Li, E., Ueda, H.R., et al. (2006). Maintenance of self-renewal ability of mouse embryonic stem cells in the absence of DNA methyltransferases Dnmt1, Dnmt3a and Dnmt3b. Genes Cells *11*, 805–814.

Whyte, W.A., Bilodeau, S., Orlando, D.A., Hoke, H.A., Frampton, G.M., Foster, C.T., Cowley, S.M., and Young, R.A. (2012). Enhancer decommissioning by LSD1 during embryonic stem cell differentiation. Nature *482*, 221–225.

Wray, J., Kalkan, T., and Smith, A.G. (2010). The ground state of pluripotency. Biochem. Soc. Trans. *38*, 1027–1032.

Wu, M., Kwon, H.Y., Rattis, F., Blum, J., Zhao, C., Ashkenazi, R., Jackson, T.L., Gaiano, N., Oliver, T., and Reya, T. (2007). Imaging hematopoietic precursor division in real time. Cell Stem Cell *1*, 541–554.

Ying, Q.L., Nichols, J., Chambers, I., and Smith, A. (2003). BMP induction of Id proteins suppresses differentiation and sustains embryonic stem cell self-renewal in collaboration with STAT3. Cell *115*, 281–292.

Ying, Q.L., Wray, J., Nichols, J., Batlle-Morera, L., Doble, B., Woodgett, J., Cohen, P., and Smith, A. (2008). The ground state of embryonic stem cell self-renewal. Nature *453*, 519–523.

Zong, C., Lu, S., Chapman, A.R., and Xie, X.S. (2012). Genome-wide detection of single-nucleotide and copy-number variations of a single human cell. Science *338*, 1622–1626.

Zwaka, T.P., and Thomson, J.A. (2005). Differentiation of human embryonic stem cells occurs through symmetric cell division. Stem Cells *23*, 146–149.